Modeling of Particle Growth and Morphology in the Gas Phase Polymerization of Butadiene. II. Simulation and Discussion

JUNZI ZHAO, JIANZHONG SUN, QIYUN ZHOU, ZUREN PAN

Department of Chemical Engineering, Zhejiang University, Hangzhou 310027, People's Republic of China

Received 9 May 2000; accepted 28 August 2000

ABSTRACT: The improved multigrain model was used to simulate the gas phase polymerization of butadiene catalyzed by low-, medium-, and high-activity catalysts, respectively. For the low-activity catalyst, the mass and heat transfer resistances in the particle were negligible. The morphology of the polymeric particles was uniform. For the medium-activity catalyst, the overall mass transfer effectiveness was $> 90\%$, the maximal temperature rise was 8K, and the heat transfer resistance in the particle was negligible. Mass transfer resistance does not affect the morphology of product particle significantly. For the high-activity catalyst, the overall mass transfer effectiveness was within the range of 70–96%, the morphology of the product particle was affected by the mass transfer resistance to some extent. The maximal temperature rise was 21K; the heat transfer resistance in the particle was negligible as well. However, there was some severe mass transfer resistance in the particle, and the maximal temperature rise was $\leq$ 30K for the large catalyst particle with the same activity. Thus, the polymeric particle morphology was comparatively poor, with the occurrence of particle softening and sticking. © 2001 John Wiley & Sons, Inc. J Appl Polym Sci 81: 730–741, 2001

Key words: butadiene; gas phase polymerization; particle growth; morphology; simulation

INTRODUCTION

Simulations of gas phase polymerization of butadiene catalyzed by low-, medium-, and high-activity catalysts were performed, respectively, using the improved multigrain model. The simulations include mainly the effects of reaction conditions and the properties of catalysts on the growth rate of polymeric particle, heat and mass transfer resistance, and the morphology of the polymeric particle.

Correspondence to: J. Sun.

Contract grant sponsor: National Natural Science Foundation of China; contract grant number: 29876035.

Journal of Applied Polymer Science, Vol. 81, 730–741 (2001)

RESULTS AND DISCUSSION OF SIMULATION

Simulation of Low-Activity Catalyst

Simulations are made with the gas phase polymerization of butadiene carried out by Junzi et al. Both the main catalyst and the cocatalyst are supported on silica. A reversible initiation mechanism of the active sites by monomer was proposed for the polymerization, and the relevant reaction parameters and kinetic constants are presented in Tables I and II.[1]

Effect of Temperature

Simulations of the effect of temperature on polymerization rate are shown in Figure 1. The sim-

Table I Reaction Conditions

p_{BD} (atm)	1.5–3.0
T_b (°C)	40–70
M_b (mol/L)	0.0607–0.1054
C_0^* (mol Nd/g cat)	3×10^{-5}

ulations are clearly in good agreement with the experimental results.

For the supported catalyst, the value of the overall polymerization rate, as well as the shape of its curve, depend on many chemical and physical factors. There are generally three types of overall polymerization rate curve: acceleration type, decay type, and hybrid type. The physical factors include the mass and heat transfer resistance in the polymer particle boundary layer and in the polymeric particle itself, whereas the chemical factors include the initiation of the active sites, propagation, and deactivation of the active sites. Moreover, the physical properties of the catalyst, including particle size, porosity, and the loading of active sites, and reaction conditions, such as temperature and monomer pressure, will affect the heat and mass transfer resistance, and thus the shape of the curve of the overall polymerization rate.

The mass transfer in the polymeric particle includes two procedures: first in the interstices between the microparticles and then within the microparticles. Thus, the overall monomer transfer effectiveness is defined as

$$\eta_{macro} = \frac{\int_v [M]_c[C^*]dV}{[M_{eq,s}]_{M_b}\int_v [C^*]dV} \quad (1)$$

where $[M_{eq,s}]_{M_b}$ is the monomer concentration of sorption equilibrium at the surface of the macroparticle corresponding $[M]_b$ and $[M]_c$ is the monomer concentration at the catalyst surface.

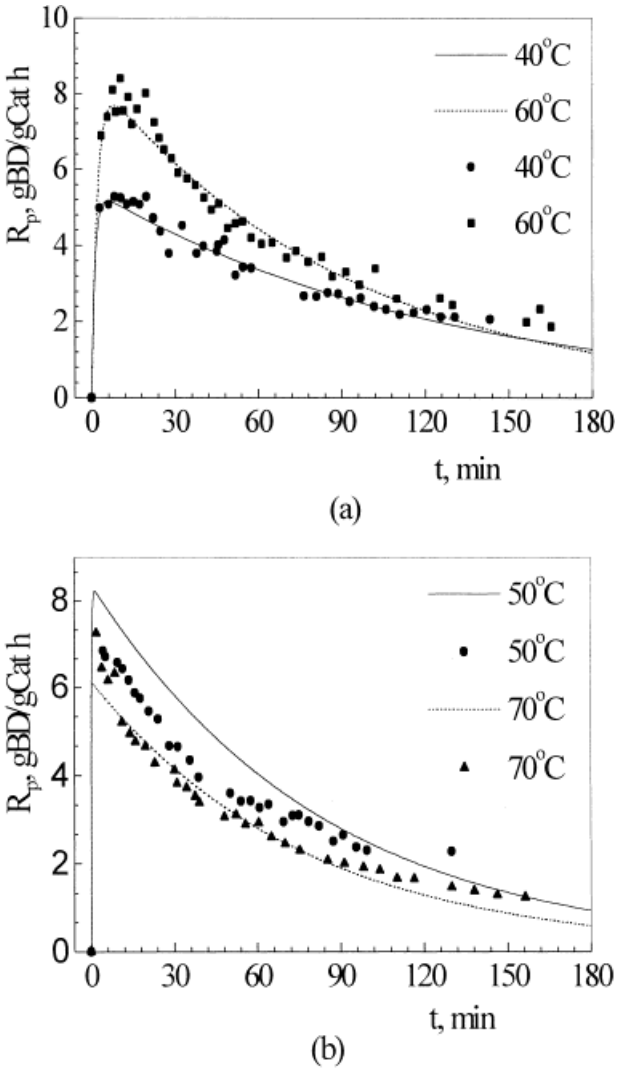

Figure 1 Comparison of the experimental results (dots) and simulation results (lines) at < 2 atm. (a) 40° and 60°C; (b) 50° and 70°C.

Figure 2 demonstrates the overall monomer transfer effectiveness for various temperatures of < 2 atm. It is shown that all η_{macro} are > 99.8%,

Table II Rate Constants of Elementary Reactions in the Intrinsic Kinetic Model

T (°C)	k_f (10^{-3} L polymer mol^{-1} s^{-1})	k_b (10^{-3} s^{-1})	k_p (L polymer mol Nd^{-1} s^{-1})	k_d (10^{-3} s^{-1})
40	7.2	6.1	1.69	28.22
50	49.9	18.8	1.99	33.21
60	9.6	1.2	2.30	38.39
70	270.9	71.7	2.39	39.90

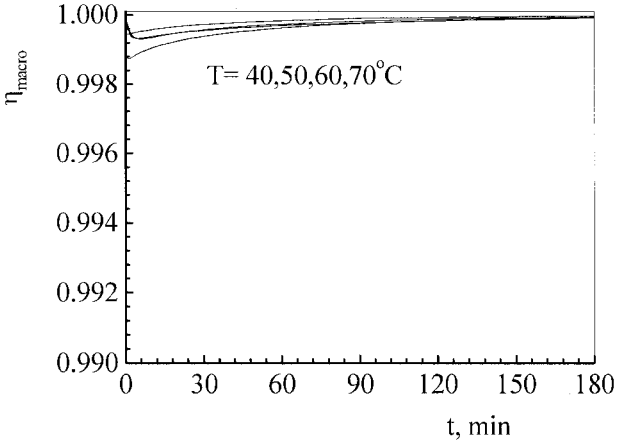

Figure 2 Overall mass transfer effectiveness factor versus time (2 atm).

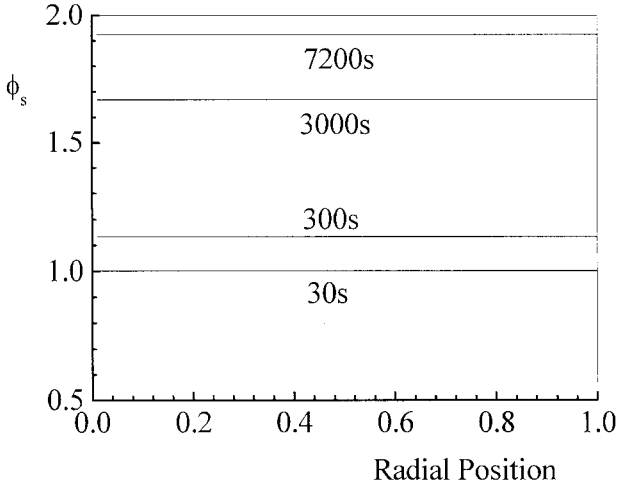

Figure 4 Profiles of microparticle growth factor at 30, 300, 3000, and 7200 s (50°C, 2 atm).

indicating that mass transfer resistance is negligible for the catalyst of low activity, in both the macroparticle and the microparticle. Practical simulations indicate that the mass transfer resistance in the polymeric particle boundary layer is also negligible.

The temperature rise of the polymeric particle versus time is shown in Figure 3, with T_c and T_b the temperatures at the center of the particle and the bulk of the gas phase, respectively. It is shown that the maximal temperature rise is only 0.025K for the low-activity catalyst. This indicates that the heat transfer resistance is negligible both in the macroparticle and at the external layer and that the temperature of the polymeric particle is almost equal to that in the reactor.

From the above analysis, it may be concluded that there is nearly no transfer resistance in the polymeric particle, and that the polymerization is controlled by kinetics for the low-activity catalyst. Thus, the growth factor of the microparticles and the local void fraction are uniform across the macroparticle, and the local void fraction remains nearly the value of the original catalyst, as demonstrated in Figures 4 and 5.

Effect of Monomer Pressure

The effect of monomer pressure on polymerization rate at 50°C is presented in Figure 6. Similarly, increasing monomer pressure does not lead to a serious temperature rise in the polymeric particle. Practical simulations indicate that the maximal temperature rise is only 0.08K at < 5 atm. The morphology of the polymeric particle, includ-

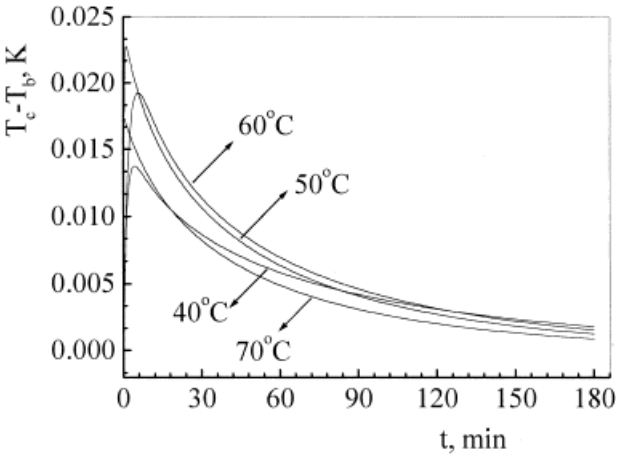

Figure 3 Temperature rise of the polymeric particle ($p = 2$ atm).

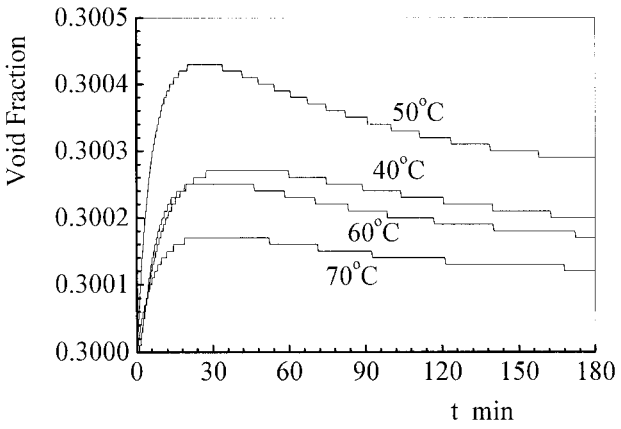

Figure 5 Predicted overall void fraction for growing polymer particle vs time ($p = 2$ atm).

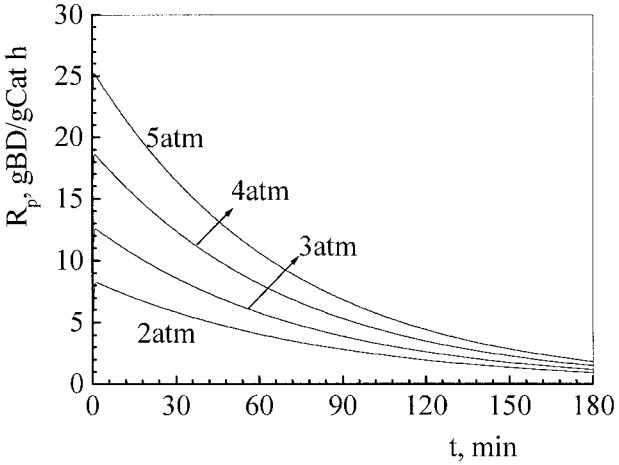

Figure 6 Effect of monomer pressure on polymerization rate at 50°C.

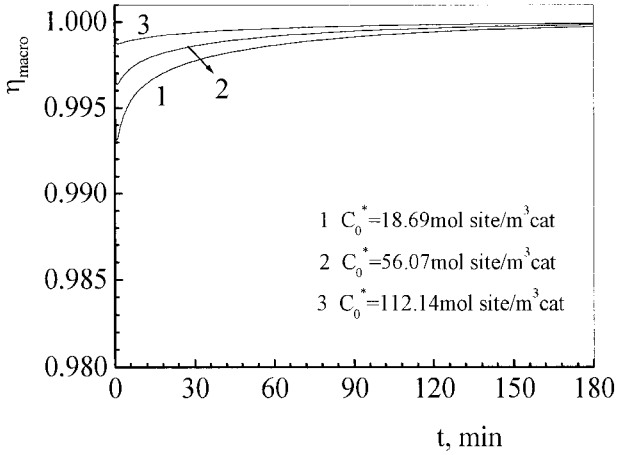

Figure 8 Overall macroparticle mass transfer effectiveness at different active site loading (50°C, 2 atm).

ing the distribution of the growth factor of the microparticles and the local void fraction across the macroparticle, was not affected by monomer pressure for this type of catalyst because increasing monomer pressure can diminish mass transfer resistance in gas phase polymerization.

Effect of Loading of Active Sites

For the supported catalyst, increasing the loading of the active sites generally leads to a high polymerization rate. Clearly, overloading of the active sites will lead to inefficient usage. Various investigators have observed that the yield per gram of transitional metal decreased with loading, hyperbolically or even exponentially. This may result from clustering or pore blockage, or simply when the reaction becomes diffusion controlled.[3]

For polymerization of olefins, almost all catalysts employed today have site concentrations within the range of 10^{-5}–10^{-4} mol/g cat.[3] In the above simulations, the site concentration is 3×10^{-5} mol/g cat. The simulations shown in Figures 7 and 8 are made for two cases that have site concentrations of 9×10^{-5} and 1.8×10^{-4} mol/g cat. Figure 8 shows that the reaction is still controlled by kinetics, even if loading of the active sites becomes 6 times its original value.

Thus, polymerization rate increases proportionally with the loading of active sites. Moreover, increasing the loading of active sites does not lead to a serious temperature rise in the polymeric particle. The morphology of the polymeric particle

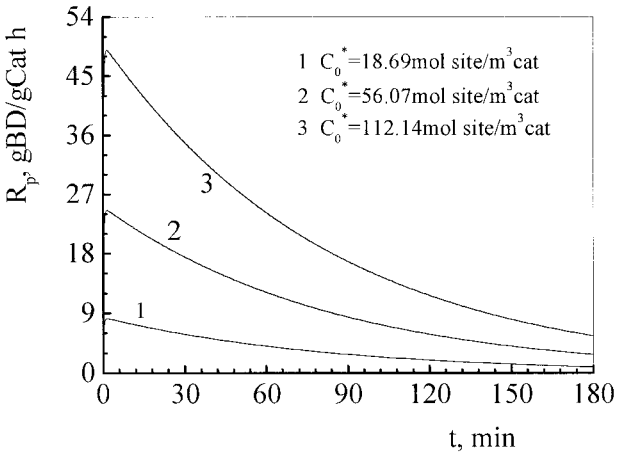

Figure 7 Effect of active site loading on polymerization rate (50°C, 2 atm).

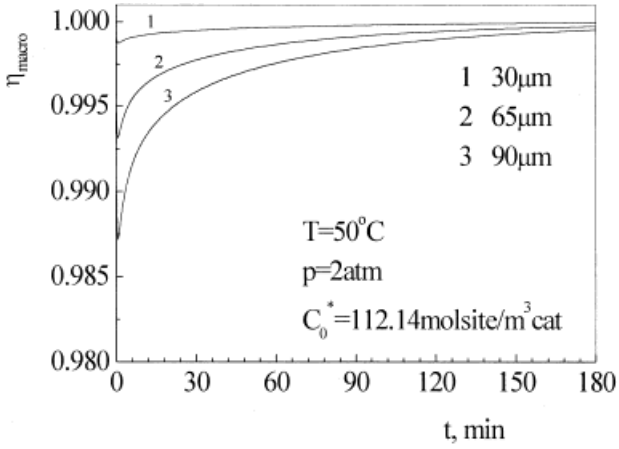

Figure 9 Overall monomer transfer effectiveness for catalyst particles of different diameters.

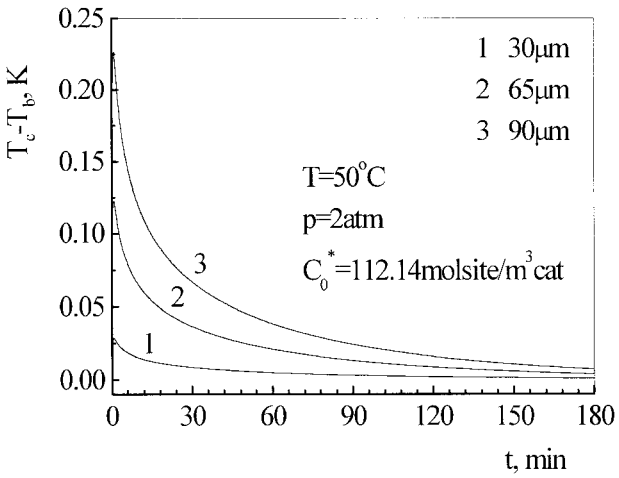

Figure 10 Temperature rise for catalyst particles of different diameters.

is also not significantly affected by the site concentration.

Effect of Size of Catalyst Particle

The size of the catalyst particle may also exert significant effects on polymerization behavior. With a high-activity catalyst, serious transfer resistance exists in the large catalyst particle size resulting in the change of the shape of the rate curve from a decay type to a hybrid type. But for gas phase polymerization of butadiene catalyzed by a low-activity catalyst, the size of the catalyst particle does not affect the mass transfer in the polymer particle significantly, as shown in Figure 9.

For gas phase polymerization, the heat transfer in the large catalyst particle is always a consideration that warrants attention. In the polymerization of olefins, there is a significant temperature rise in large particles of high activity, which might approach the softening or melting point of the polymer, resulting in particle softening, agglomeration, and sticking.[2] Figure 10 demonstrates the tendency toward a more pronounced temperature rise in the larger particle. However, the value of the temperature rise is actually small, because the activity of the catalyst is relatively low.

Table III Parameters for Butadiene Gas-Phase Polymerization*

T (K)	293–323
P (atm)	2–2.7
k_p^0 (L/mol sites)	1.6×10^4
E_p (J/mol)	2.4×10^4
k_d^0 (L/s)	1.5×10^4
E_d (J/mol)	5.0×10^4
ρ_{cat} (kg/m^3)	623
C_0^* (mol sites/kg cat)	1.8×10^{-1}

* Carried out by K.H. Reichert.

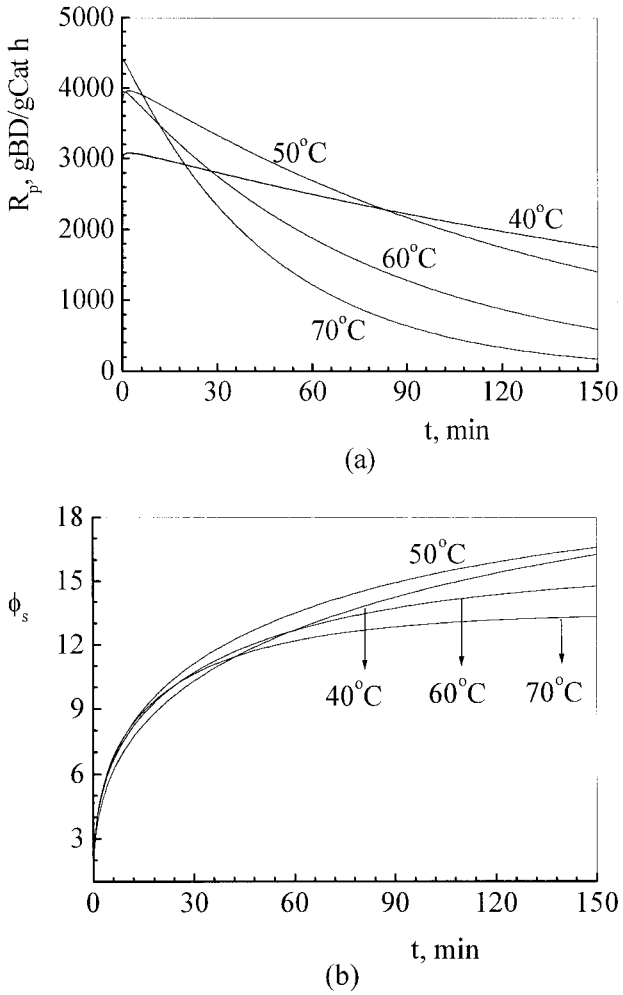

Figure 11 Effect of temperature on polymerization rate (a) and on polymeric particle growth rate (b) < 2 atm.

Several conclusions may be drawn from these findings: for the low-activity catalyst used in this simulation whose overall polymerization rate constant is $\sim$ 20 L/mol site s, the transfer resistance is negligible, and the reaction is controlled by kinetics. The morphology of the polymer particle is uniform and the overheating of the particle may not occur.

Simulation of Medium-Activity Catalyst

K.H. Reichert carried out the gas phase polymerization of butadiene catalyzed by a medium-activ-

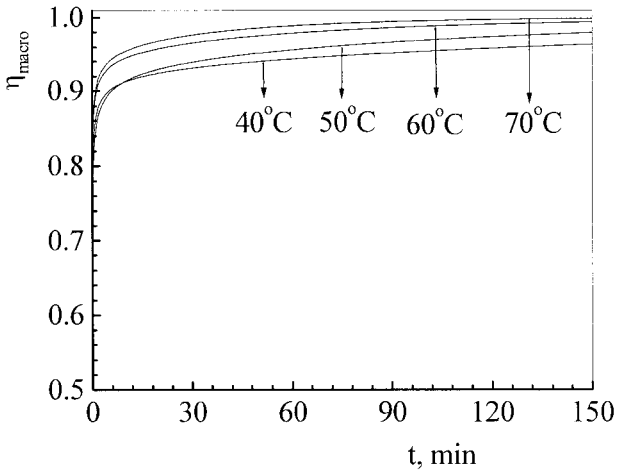

Figure 12 Comparison of overall monomer transfer effectiveness at different temperature (2 atm).

ity catalyst whose active sites are initiated instantaneously. The relevant reaction parameters and kinetic constants are presented in Table III.[5,6]

The effects of temperature on polymerization rate and the growth rate of the polymeric particle are presented in Figure 11. It can been seen that the activity of the catalyst is relatively high, and the polymeric particle may grow $\leq$ 18 times the original size of the catalyst particle.

Figures 12 and 13 demonstrate that the overall mass transfer effectiveness decreases to 90% at the beginning of polymerization; the mass transfer resistance is not serious for the medium-activity catalyst. With time, the mass transfer resistance decreases, producing flattened profiles in

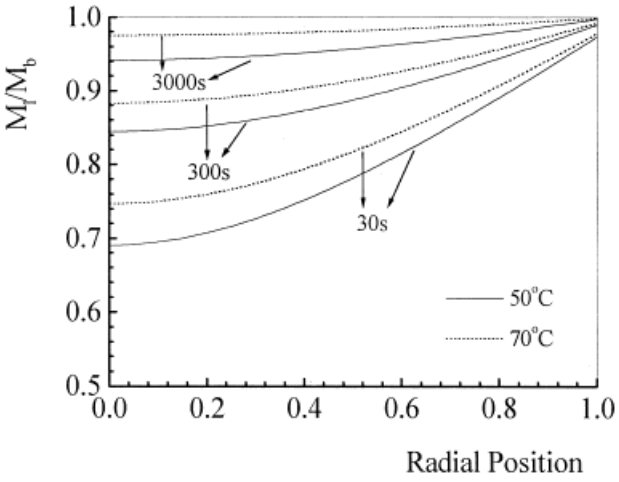

Figure 13 Profiles of macroparticle monomer concentration for 50° and 70°C (2 atm).

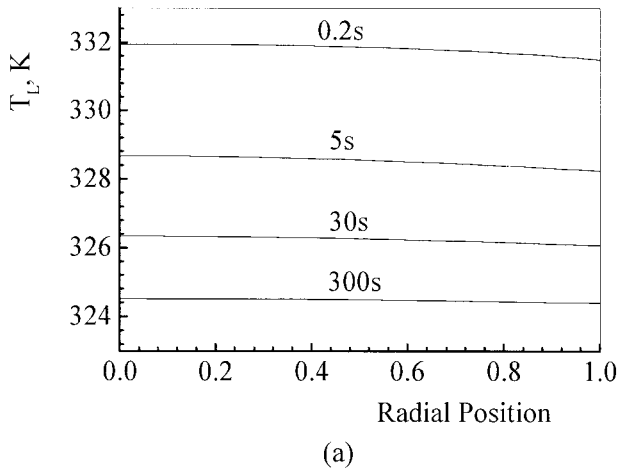

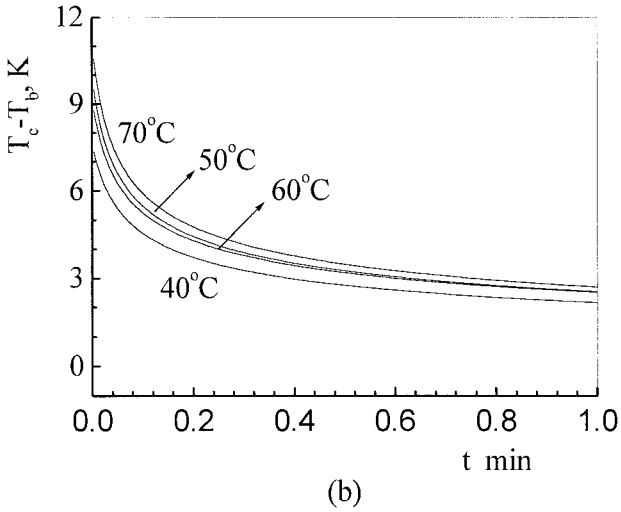

Figure 14 Modeling of macroparticle heat transfer resistance. (a) Profiles of temperature at 0.5, 5, 30, 300, s at 50°C, 2 atm; (b) temperature rise vs. time at 40, 50, 60, 70°C at $<$ 2 atm.

the monomer concentration. Figure 13 also shows that the monomer concentration gradient in the external layer, ΔM, is about 5% at the beginning of the polymerization, indicating that the mass transfer resistance in the external layer is not also serious. With time, the mass transfer resistance in the external layer gradually becomes negligible, as the area for the mass transfer increases and the polymerization rate decays.

It also can be seen in Figure 11 that at $<$ 2 atm, the polymerization rate at 70°C is lower than that at 50°C, which is unexpected. The reason for this phenomenon is that the activation energy for deactivation of the active sites is greater than that for propagation (Table III). Thus, when the temperature is increased k_d increases to a greater

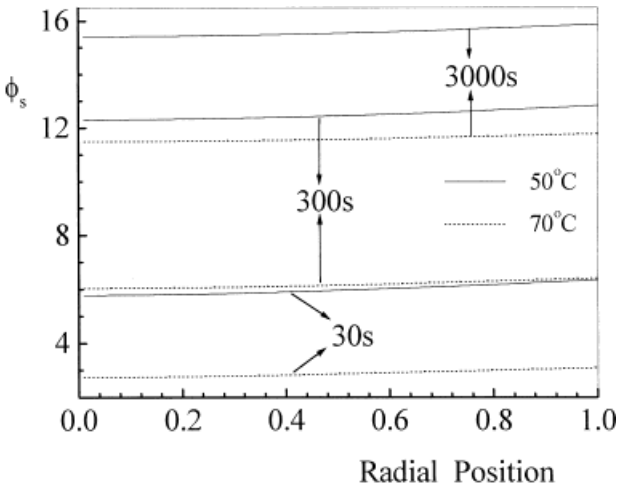

Figure 15 Profiles of microparticle growth factors at 30, 300, 30,000 s for reactions at 50° and 70°C at < 2 atm.

extent than k_p, leading to the decrease of the polymerization rate at higher temperature. The mass transfer resistance is affected by this effect directly, as demonstrated in Figure 12. The mass transfer resistance at the higher polymerization rate is more serious than that at lower polymerization rate.

Figure 14 demonstrates that for the medium-activity catalyst, the maximal temperature rise in the polymer particle is up to ~ 8K at the beginning of polymerization, although the heat transfer resistance in the polymer particle is also negligible. The temperature in the polymer particle decreases quickly to the same temperature as that in the reactor itself, as the polymerization rate decays gradually and the area for the heat transfer increases with time. Thus, particle softening and agglomeration will not occur.

For slurry polymerization, the mass transfer resistance is significant (with the value of D_l within the range of 10^{-6}–10^{-5} cm^2/s); Hutchinson's simulations indicated that[4] the growth factor of the microparticles in the outer shell is 60% larger than that in the interior shells for a catalyst of similar activity. This effect is not as significant for gas phase polymerization of butadiene catalyzed by a catalyst of similar activity (Fig. 15), because the mass transfer resistance is relatively small, with (the value of D_l within the range of 10^{-3}–10^{-4} cm^2/s).

The effect of reaction conditions on the local void fraction of the macroparticle is presented in Figure 16. At the beginning of polymerization, the difference of the growth rate of the microparticles across the macroparticle leads to an uneven distribution of the void fraction. The microparticles in the outer shells grow at higher rate than do those in the interior shells, leading to separation of microparticle layers and an increased void fraction. However, microparticle growth rates become more uniform across the particle as the concentration gradients disappear with time; the void fraction decreases back toward the value of the original catalyst. The effect of temperature on the overall void fraction may be reflected from the effect of the polymerization rate: a higher polymerization rate results in a higher overall void fraction, whereas a lower polymerization rate results in a lower overall void fraction, which is also similar to the case in slurry polymerization of olefins.

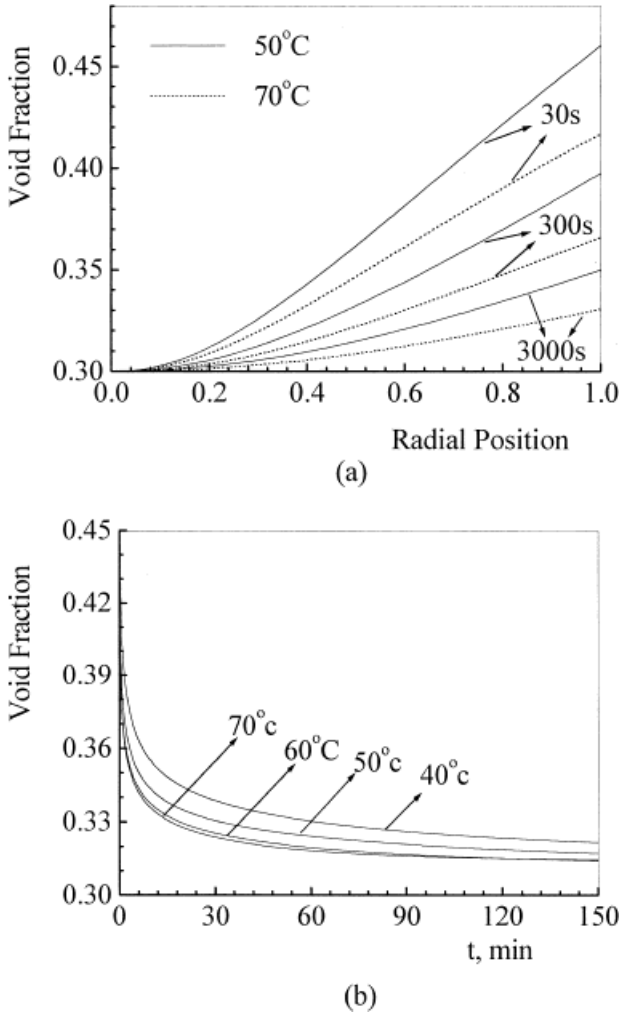

Figure 16 Predicted void fraction for growing polymer particle. (a) radial profiles at 30, 300, 3000 s for reactions at 50° and 70°C at < 2 atm; (b) overall void fraction vs. time.

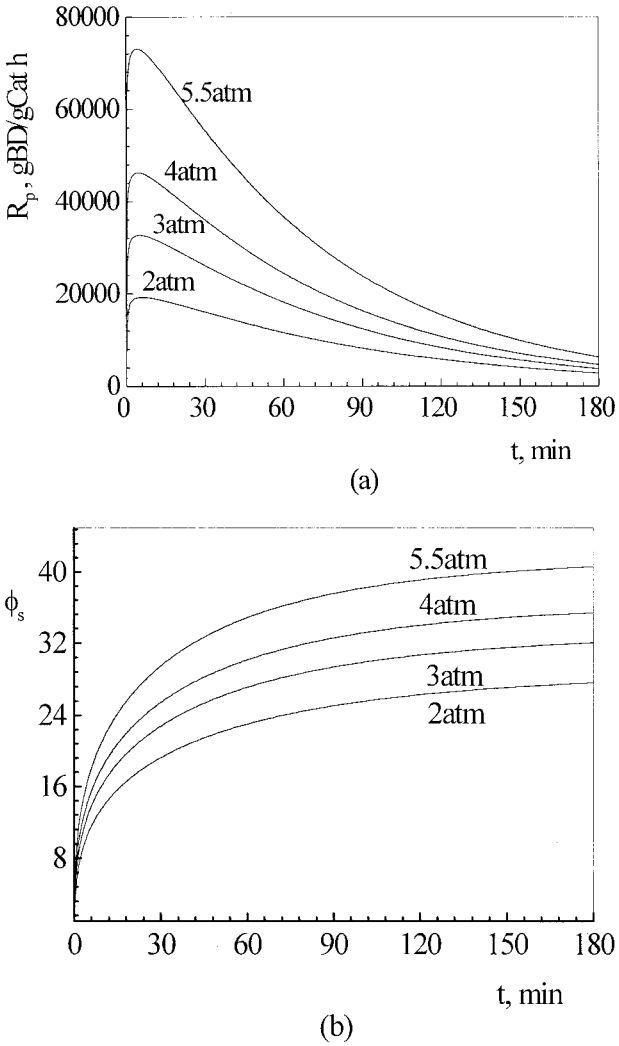

Figure 17 Curve of polymerization rate (a) and polymer particle growth rate (b) for high-activity catalyst at 50°C.

Simulation of High-Activity Catalyst

To simulate the behavior of gas phase polymerization of butadiene completely, a high-activity catalyst, similar to the activity of the high-activity catalysts used in heterogeneous polymerization of propylene, is applied to the gas phase polymerization of butadiene. The polymerization has the same kinetic model as that of the polymerization discussed for the low-activity catalyst described earlier. The relevant reaction parameters and propagation rate constant k_p are tabulated in Table IV, and the other three kinetic rate constants k_d, k_f, and k_b, which are related to the initiation and deactivation of the active sites, have the same values as those of their counterparts described in the section, Simulation of Low-Activity Catalyst.

Table IV Modeling Parameters for Gas-Phase Polymerization of Butadiene With High-Activity Catalyst

P (atm)	2–5.5
T_b (K)	323.15
M_b (mol/L)	0.0756–0.205
k_p (L/mol site)	6000
C_0^* (mol site/m^3 cat)	18.69

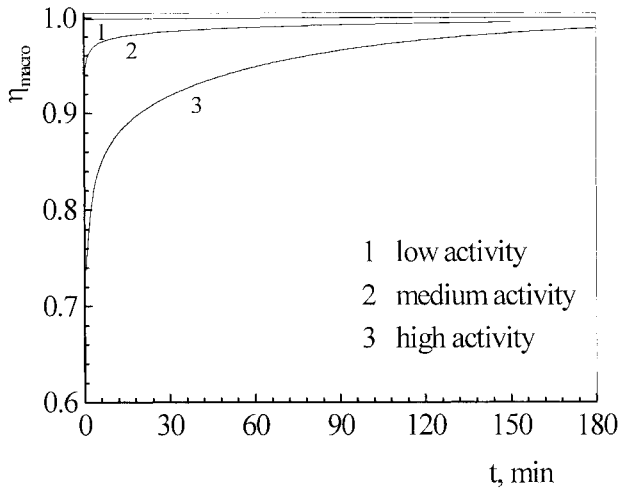

Figure 18 Comparison of mass transfer effectiveness of low-, medium-, and high-activity catalysts (50°C, 2 atm).

Effect of Monomer Pressure

The effect of monomer pressure on polymerization rate and the growth rate of the polymeric particle

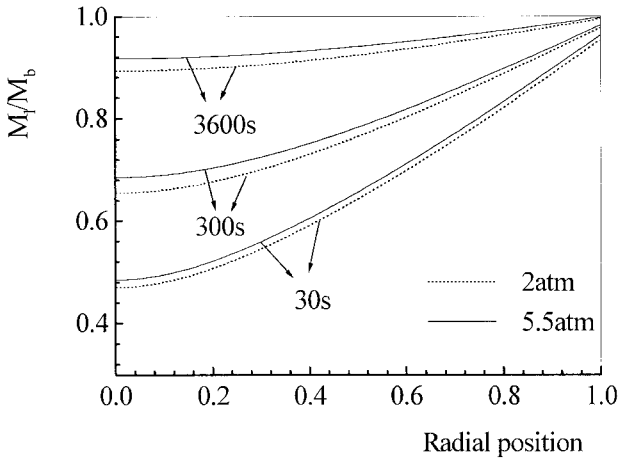

Figure 19 Profiles of macroparticle monomer concentration < 2 and 5.5 atm (50°C).

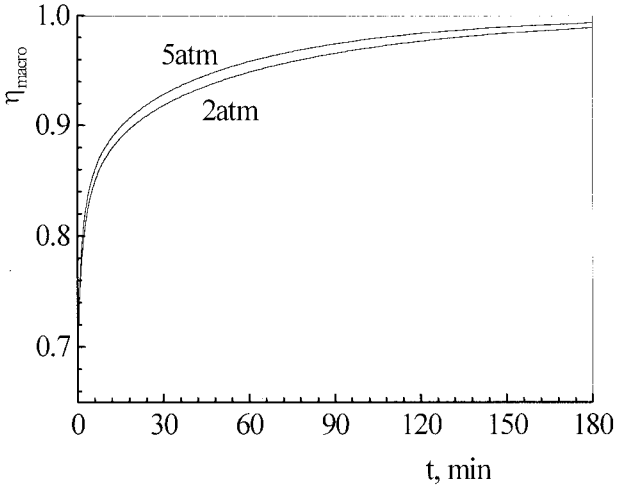

Figure 20 Effect of pressure on monomer transfer effectiveness at 50°C for high-activity catalyst.

is presented in Figure 17. It can been seen that the activity of the catalyst is so high that the polymer particle may even grow ≤ 40 times the original size of the catalyst particle.

For a high-activity catalyst, the extent to which the mass and heat transfer resistance affect polymerization behavior, including polymerization rate, molecular weight, and distribution is always a primary concern. Thus, the overall monomer transfer effectiveness for the low-, medium-, and high-activity catalysts are compared in Figure 18. It can be seen that the overall monomer mass transfer effectiveness for the high-activity catalyst is within a lower range of 70–96% throughout polymerization, as compared with the low- and

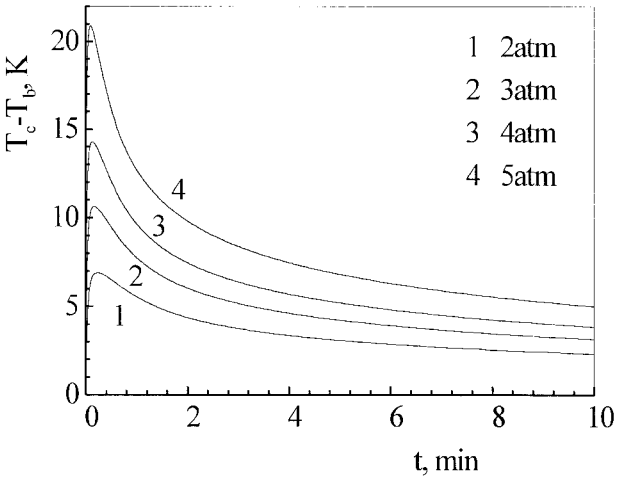

Figure 21 Effect of pressure on growing particle temperature rise (50°C).

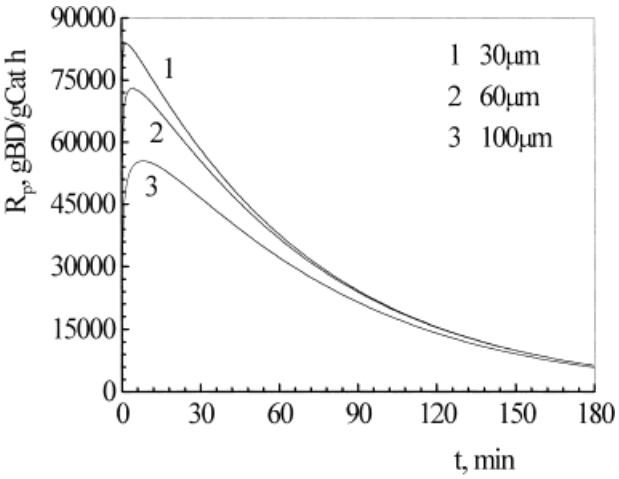

Figure 22 Effect of catalyst particle diameter on polymerization rate.

medium-activity catalyst. Figure 19 also demonstrates that at the beginning of the polymerization, the monomer concentration gradient ΔM in the external layer is less than 10%, which indicates that the mass transfer resistance in the external layer becomes relatively pronounced, but not serious. Figure 20 shows that the effect of decreasing the mass transfer resistance by increasing monomer pressure is not obvious. Thus, the mass transfer resistance for the high-activity catalyst affects the shape of the curve of the polymerization rate and the morphology of the polymeric particle to a greater extent than do the low, medium activity catalysts. But the effect is not so significant as in slurry polymerization with catalyst of similar activity.

For this high-activity catalyst, increasing monomer pressure, which will not affect the mass transfer resistance and the morphology of the polymeric particle significantly, can result in a serious temperature rise in the polymeric particle. The maximal temperature rise in the particle < 2 atm is 7K, while the temperature rise under 5.5 atm is ≤ 21K, as demonstrated in Figure 21. The temperature rise decreases to $<$ 5K in 10 min, as the mass transfer resistance is relatively serious, leading to a lower monomer concentration in the particle at the beginning of polymerization; the polymerization rate decays gradually, and the area for the heat transfer increases with time. Thus, particle softening and agglomeration will not occur. This analysis is made for catalyst particles of 60-μm diameter. It may be concluded that the general particle will not soften or agglomerate for gas phase polymerization of butadiene.

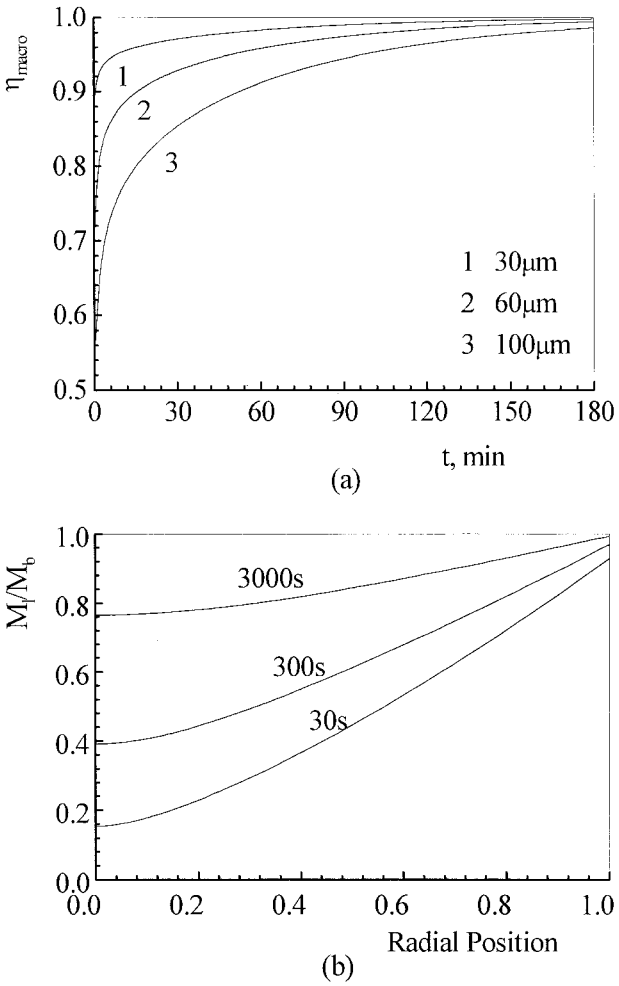

Figure 23 Effect of catalyst diameter on mass transfer resistance. (a) mass transfer effectiveness for catalysts of different diameter; (b) monomer concentration profiles for catalyst of diameter 100 μm.

Effect of the Size of Catalyst Particle

In gas phase polymerization of olefins for the high-activity catalyst, serious mass transfer resistance occurs in the large particle. Figure 22 demonstrates the effect of catalyst diameter on the rate of polymerization. The shape of the polymerization rate curve for the large catalyst particle has some characteristics of the acceleration type, indicating the existence of serious mass transfer resistance qualitatively. Figure 23 demonstrates this point quantitatively.

The serious mass transfer resistance in the macroparticle results in the uneven polymerization rate across the macroparticle. Thus, the local void fraction is also uneven, as shown in Figure 24.

The distribution of growth factors of microparticles across the macroparticle is presented in Figure 25. It can been seen that the difference of the growth factors of microparticles in the internal and external shell is large at the beginning of polymerization because of the serious mass transfer resistance. The growth factor of microparticles in the outermost shell is 2 times that at the center of the macroparticle. The difference becomes less severe gradually with time, but it still remains at 25% at the end of polymerization.

As mentioned above, overheating will not occur for the general polymer particle for the gas phase polymerization of butadiene. However, this is not the case for large particles. Figure 26 indicates that the maximal temperature rises to $\leq$ 30K at the beginning of polymerization, which will result in softening of the particle. This phenomenon is

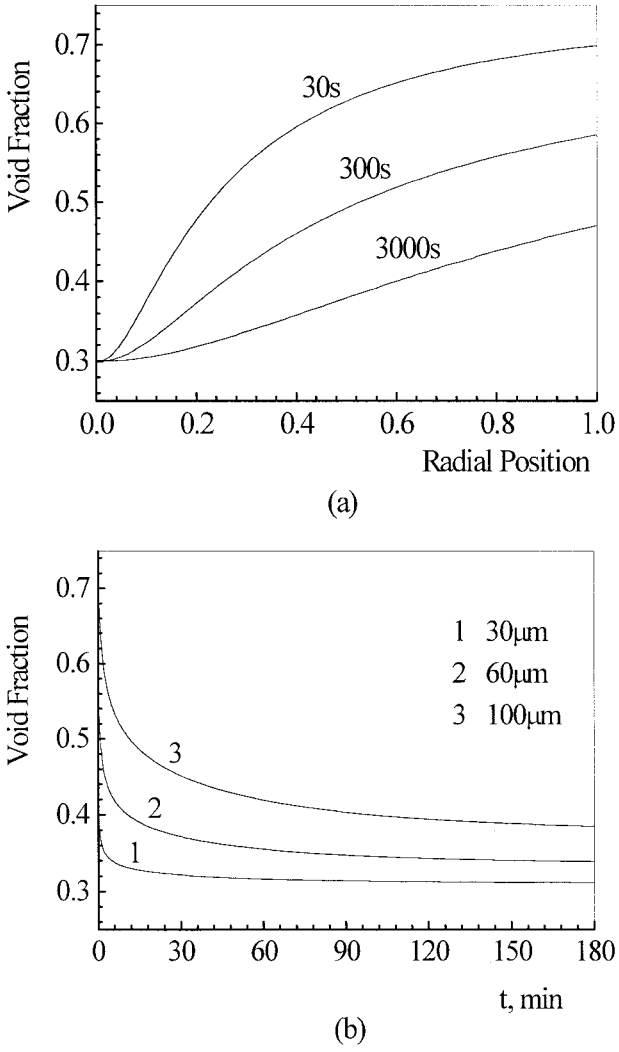

Figure 24 Effect of catalyst diameter on particle void fraction. (a) Radial profiles at 30, 300, 3000 s (dc = 100 μm) (b) overall void fraction vs. time.

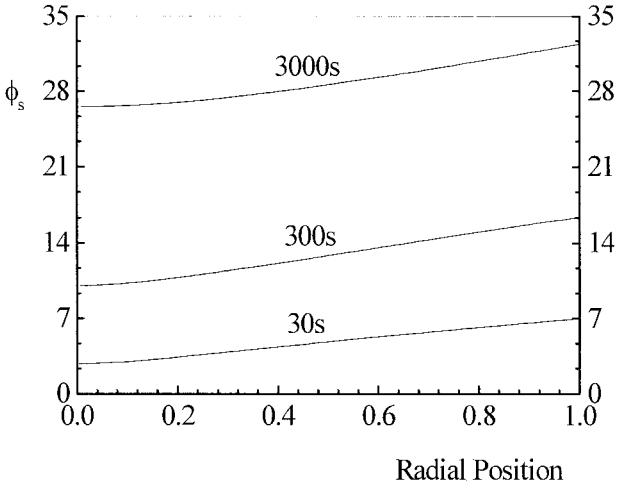

Figure 25 Profiles of microparticle growth factor for large catalyst particle (dc = 100 μm).

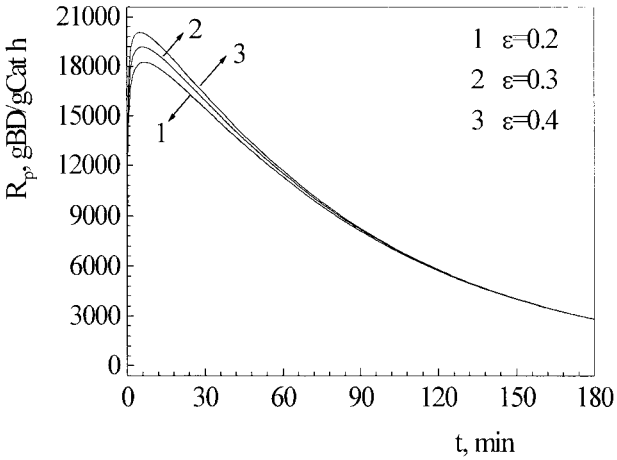

Figure 27 Effect of catalyst void fraction on polymerization rate.

independent of the capacity of heat removal of the reactor itself. Furthermore, the morphology of the polymer product over the large catalyst particle is poor. Thus, the large-diameter catalyst particle is undesirable in preparation of the catalyst.

Effect of Void Fraction of Catalyst Particle

It is useful to examine the effect of the initial void fraction of the catalyst particle on polymerization behavior, because the diffusivity within the macroparticle is proportional to the void fraction,[4] as stated above. The above simulations are for the catalyst particle with $\epsilon_0 = 0.3$. Here simulations are made for the catalyst particle with $\epsilon_0 = 0.2$ and 0.4, in order to examine the effects of ϵ_0 on polymerization rate, the overall mass transfer effectiveness, and the overall void fraction of the product particle, which are presented in Figures 27–29. The results indicate that the mass transfer resistance increases and the polymerization rate decreases as ϵ_0 decreases. However, ϵ_0 does not affect the polymerization behavior as significantly as does the size of the catalyst particle does.

Figure 29 demonstrates that the overall void fraction of the product particle is dependent mainly on the initial void fraction of the catalyst particle ϵ_0. Although the catalyst of $\epsilon_0 = 0.2$ has the lowest final void fraction, it shows the largest increase relative to the initial value. This is because of the more severe mass transfer limitations for the low-porosity particle.

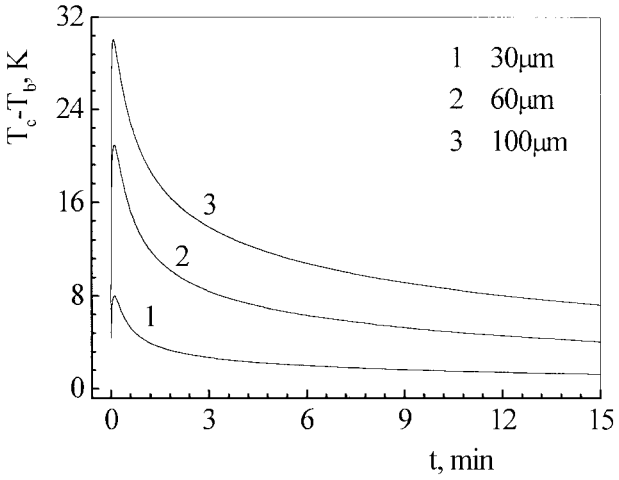

Figure 26 Effect of catalyst diameter on temperature rise of growing polymer particle.

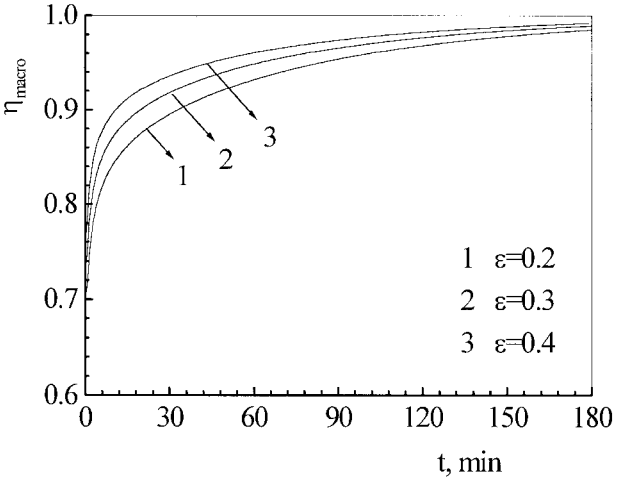

Figure 28 Effect of catalyst void fraction on overall mass transfer effectiveness.

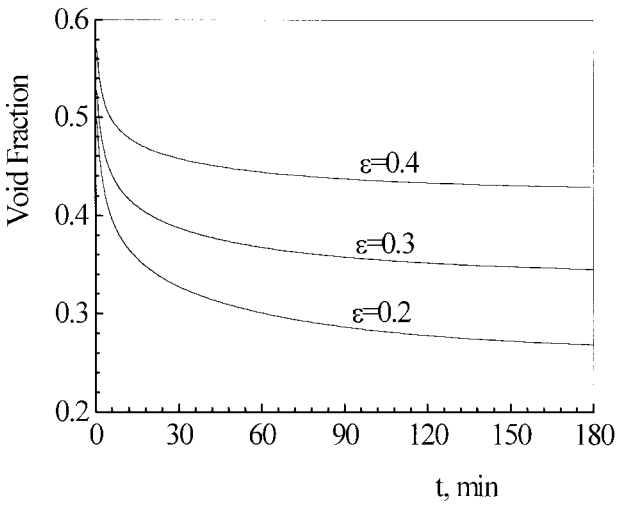

Figure 29 Effect of catalyst void fraction on overall void fraction of polymeric particle.

CONCLUSIONS

Simulations were made of the gas phase polymerization of butadiene catalyzed by low-, medium-, and high-activity catalysts, respectively, using the improved multigrain model. The following conclusions may be drawn:

1. For the low-activity catalyst, the polymerization was controlled by kinetics. The morphology of the polymeric particle was uniform.
2. For the medium-activity catalyst, the overall mass transfer effectiveness was $> 90\%$; the maximal temperature rise was 8K, and the heat transfer resistance in the particle was negligible. Mass transfer resistance does not significantly affect the morphology of the product particle.
3. For the high-activity catalyst, the overall mass transfer effectiveness was 70–96%; the morphology of product particle was affected by the mass transfer resistance to some extent. The maximal temperature rise was 21K; the heat transfer resistance in the particle was also negligible. However, some severe mass transfer resistance in the particle was demonstrated, and the maximal temperature rise was $\leq$ 30K for large catalyst particle with the same activity. Thus, the polymeric particle morphology becomes comparatively poor, and particle softening and sticking will occur.

NOMENCLATURE

C^*	concentration of active sites, mol site m^{-3} cat or mol site g^{-1} cat
C_0^*	concentration of active sites at time zero, mol site m^{-3} cat or mol site g^{-1} cat
D_b	bulk diffusivity of monomer, $cm^2\ s^{-1}$
D_l	effective diffusivity in the macroparticle, $cm^2\ s^{-1}$
D_s	effective diffusivity in the microparticle, $cm^2\ s^{-1}$
d_p	diameter of the polymer particle, μm
E_A or E_p	activation energy for propagation, kJ mol^{-1}
k_b	rate constant of the deformation of active centers, s^{-1}
k_d	rate constant of deactivation of the active site, s^{-1}
k_f	rate constant of the formation of active centers, L polymer $mol^{-1}\ s^{-1}$
k_p	propagation rate constant, L polymer mol $site^{-1}\ s^{-1}$
M_b	bulk monomer concentration, mol L^{-1}
M_c	monomer concentration at catalyst surface, mol L $polymer^{-1}$
ΔM	monomer concentration gradient in the external layer
R_p	overall polymerization rate, g BD g $cat^{-1}\ h^{-1}$
T_b	temperature in the reactor, K

GREEK SYMBOLS

ϵ_0	void fraction of catalyst particle
$\epsilon_l(L_l,t)$	void fraction of macroparticle
η_{macro}	overall monomer mass transfer effectiveness
ρ_{cat}	density of catalyst particle, kg m^{-3}
ϕ_s	microparticle growth factor

REFERENCES

1. Junzi, Z.; Jianzhong, S.; Qiyun, Z.; Zuren, P. J Chem Ind Eng (China), to appear, 2001.
2. Floyd, S.; Choi, K. Y.; Taylor, T. W.; Ray, W. H. J Appl Polym Sci 1986, 32, 2935.
3. Floyd, S.; Heiskanen, T.; Taylor, T. W. J Appl Polym Sci 1987, 33, 1021.
4. Hutchinson, R. A.; Chen, C. M.; Ray, W. H. J Appl Polym Sci 1992, 44, 1389.
5. Eberstein, C.; Garmatter, B.; Reichert, K. H.; Sylvester, G. Chem Ingen Technik 1996, 68, 820.
6. Jianzhong, S.; Eberstein, C.; Reichert, K. H. J Appl Polym Sci 1997, 64, 203.